ATLANTIS PRESS
Advances in Engineering Research (AER), volume 131
3rd Annual International Conference on Electronics, Electrical Engineering and Information Science (EEEIS 2017)

Image Edge Detection Algorithm Based on Interpolation Wavelet Decomposition

Zhi-Guo ZHANG [a,*], Xi ZHENG, Li LI

University of Electronic Science and Technology of China, Chengdu, 611730, China

[a]zhiguozhang@uestc.edu.cn

[*]Corresponding author

Keywords: Image Edge Detection, Interpolation Wavelet, Interpolation Filter, Mallat Pyramidal Algorithm.

Abstract. In digital image processing, classic wavelet algorithm often has difficulties in obtaining accurate wavelet coefficients by using continuous integral formula. Hence, clear and accurate edges of images cannot be detected in the classic wavelet algorithm. To deal with this problem, a new algorithm is proposed to detect image edges with sparse representation of interpolation wavelets. By utilizing the special property that image pixel values can be considered as interpolation wavelet coefficients, interpolation dual filter is combined with Mallat pyramidal algorithm in this algorithm. Theoretical analysis and experimental results demonstrate that this algorithm can avoid integral formula for obtaining wavelet coefficients. Thus, compared to the classic one, a better edge result can be detected for the new algorithm.

Introduction

Edges can be considered as a set of pixels whose values have step or roof changes. Due to sensitivities to high- frequency signal, differential operators can effectively reflect such rapid changings. Thus, they may be one of the most important tools in traditional edge detection algorithms. However, differential operators often have difficulties in distinguishing edges accurately from noisy images since noise generally contains a mass of high-frequencies.

To solve the above-mentioned problems, Mallat proposed an effective edge detection algorithm by application of wavelets[1][2]. Since wavelet transform is an effective method to analyze signals in time-frequency, it can effectively describe sharp changes in localization of images. Hence, when wavelet transform[3-[5] is applied to image edge detection, the influence of noise can be decreased and higher precision edges are obtained. This has make wavelets become an important method for edge detection.

From then on, wavelets have been used widely in image processing. Simultaneously, many new algorithms are proposed to deal with edge detection based on some special wavelets such as omnidirectional wavelet transform[6], B-spline wavelet transform[7], and wavelet transform with morpholopy[8] or canny operator[9].

People have made great progress in application of wavelet to edge detection, but the abovementioned methods still have many shortcomings such as complex computation and low accuracy. Clearly, it follows from sampling theory that samples can be considered as coefficients of interpolation wavelets series [10]-[11]. Since pixels of images can be considered as samples of target functions, applications of interpolation wavelets to image processing can greatly improve efficiency of wavelet transform. This motivates us to detect image edges based on wavelet sampling theory. The work [11] has proposed an algorithm for constructing interpolation filters. Here, with aid of this result, a new algorithm is proposed to detect image edges by combining interpolation filters and Mallat pyramidal algorithm. In this new algorithm, wavelet coefficients are obtained from samples directly instead of inner product formula. Thus edges of images can be detected efficiently.

The Classical Wavelet Algorithm in Image Edge Detection

Assume that $\phi(x)$ and $\psi(x)$ are respectively a scaling function and its corresponding wavelet. $\{V_j\}_{j\in\mathbf{Z}}$ forms a multiresolution analysis (MRA) of $L^2(\mathrm{R})$. W_j is a wavelet space such that $V_{j+1}=V_j\oplus W_j$, where $\oplus$ denotes an orthogonal direct sum. Then for any function $f(x)\in L^2(\mathrm{R})$, we have

$$f(x)=\sum_{k\in\mathrm{Z}}\sum_{j\in\mathrm{Z}}c_k^j\psi(2^j x-k), \tag{1}$$

where $\{c_k^j\}_{k\in\mathrm{Z}}$ are wavelet coefficients such that

$$c_k^j=\left\langle f(x),\psi(2^j x-k)\right\rangle=\int_{x=-\infty}^{+\infty}f(x)\psi^*(2^j x-k)dx. \tag{2}$$

Since multidimensional wavelets can be generated by tensor product of one-dimensional wavelets, i.e. $\psi(x,y)=\psi_1(x)\psi_2(y)$, Hence, Eqs. (1) and (2) in two dimensions can be respectively expressed as

$$f(x)=\sum_{k,m\in\mathrm{Z}}\sum_{j\in\mathrm{Z}}c_{k,m}^j\psi(2^j x-k)\psi(2^j x-m) \tag{3}$$

and

$$\begin{aligned}c_{k,m}^j&=\left\langle f(x,y),\psi(2^j x-k,2^j y-m)\right\rangle\\&=\int_{x=-\infty}^{+\infty}\int_{y=-\infty}^{+\infty}f(x,y)\psi^*(2^j x-k,2^j y-m)dxdy.\end{aligned} \tag{4}$$

Clearly, it follows from edge detection theories that wavelet coefficients play a critical role in detecting image edge. Since an digital image is generally represented in form of a matrix in practice, the presentation

$$c_{k,m}^j\approx\sum_l\sum_n f(x_l,y_n)\psi^*(2^j x_l-k,2^j y_n-m)\Delta x\Delta y \tag{5}$$

is often used to replace (4) for obtaining wavelet coefficients.

According to the Riemann integral formula

$$\begin{aligned}&\lim_{\substack{\Delta x\to 0\\ \Delta y\to 0}}\sum_l\sum_n f(x_l,y_n)\psi^*(2^j x_l-k,2^j y_n-m)\Delta x\Delta y\\&=\int_{x=-\infty}^{+\infty}\int_{y=-\infty}^{+\infty}f(x,y)\psi^*(2^j x-k,2^j y-m)dxdy,\end{aligned} \tag{6}$$

equation (5) can be a good approximation of (4) for a set of enough dense samples.

However, with development of image processing, higher resolution of image edge is required in application. Equation (5) in fact has had difficulties in obtaining a good approximation. If Δx and Δy in (5) respectively denote the pixel physical intervals of an image acquisition device in horizontal and vertical direction, then (5) in the resolution of 2^j can be expressed as

$$\begin{aligned}c_{k,m}^j&\approx\sum_{k_1}\sum_{k_2}f(k_1\Delta x,k_2\Delta y)\\&\quad\times\psi^*(2^j k_1\Delta x-k,2^j k_2\Delta y-m)\Delta x\Delta y.\end{aligned} \tag{7}$$

However, when the resolution is increased to 2^{j+1}, we have

$$\begin{aligned}c_{k,m}^{j+1}&\approx\sum_{k_1}\sum_{k_2}f(k_1\Delta x,k_2\Delta y)\\&\quad\times\psi^*(2^{j+1}k_1\Delta x-k,2^{j+1}k_2\Delta y-m)\Delta x\Delta y.\end{aligned} \tag{8}$$

Suppose $\Delta x'=2\Delta x$, $\Delta y'=2\Delta y$, then (8) can be represented as

$$\begin{aligned}c_{k,m}^{j+1}&\approx\frac{1}{4}\sum_{k_1}\sum_{k_2}f(\frac{1}{2}k_1\Delta x',\frac{1}{2}k_2\Delta y')\\&\quad\times\psi^*(2^j k_1\Delta x'-k,2^j k_2\Delta y'-m)\Delta x'\Delta y'.\end{aligned} \tag{9}$$

On the other hand, it follows from (4) that

$$\begin{aligned}c_{k,m}^{j+1}&=\int_{x=-\infty}^{+\infty}\int_{y=-\infty}^{+\infty}f(x,y)\psi^*(2^{j+1}x-k,2^{j+1}y-m)dxdy\\&=\frac{1}{4}\int_{x=-\infty}^{+\infty}\int_{y=-\infty}^{+\infty}f(\frac{1}{2}x,\frac{1}{2}y)\psi^*(2^j x-k,2^j y-m)dxdy.\end{aligned} \tag{10}$$

Obviously, (7) and (9) are respectively approximations of (4) and (10), which are used to obtain

wavelet coefficients at resolution 2^j and 2^{j+1}. Compared (7) to (9), the equivalent sampling periods $\Delta x'$ and $\Delta y'$ in (9) become twice than Δx and Δy in (7). This implies that higher resolution of wavelets in image edge detection can cause larger sampling intervals $\Delta x'$ and $\Delta y'$ even if physical sampling intervals Δx and Δy are unchanged for an image acquisition device.

On the other hand, it known from Riemann integral theory that increase of Δx and Δy can lead up to a larger calculation error for approximation of (7) to (4). Thus, with resolution improvement of image edge detection, the approximation (5) of integral formula (4) cannot produce enough accurate wavelet coefficients. Conversely, in order to get accurate wavelet coefficients, the resolution of image edge detection is generally limited. Hence, classic integral method has difficulty in obtaining results of high resolution in image edge detections.

To solve the above-mentioned problem, based on Mallat pyramidal algorithm and interpolation wavelets, this paper proposes a new method to deal with image edges. Theoretical analysis demonstrates that this algorithm can avoid numerical integral formula for obtaining wavelet coefficients. Hence a better edge detect result can be obtained.

The Mallat Pyramidal Algorithm and Interpolation Wavelet

Classic Two-dimensional Mallat Pyramidal Algorithm

Assume that $\{V_j^2\}_{j\in Z}$ forms a MRA of $L^2(R^2)$, and satisfies $V_j^2 = V_{j-1}^2 \oplus W_{j-1}^2$, where

$$W_{j-1}^2 = (V_{j-1}\otimes W_{j-1}) \oplus (W_{j-1}\otimes V_{j-1}) \oplus (W_{j-1}\otimes W_{j-1}). \tag{11}$$

Let $\phi(x,y) = \phi(x)\phi(y)$ be a scaling function for the approximation space V_0^2. Then

$$\begin{cases} \psi^1(x,y) = \phi(x)\psi(y) \\ \psi^2(x,y) = \psi(x)\phi(y) \\ \psi^3(x,y) = \psi(x)\psi(y) \end{cases} \tag{12}$$

are wavelets corresponding to $\phi(x,y)$. This implies that

$$\{\phi_{j,k,m}(x,y) = 2^j\phi(2^j x-k, 2^j y-m)\}_{k,m\in Z} \tag{13}$$

and $\{\psi_{j,k,m}^1(x,y), \psi_{j,k,m}^2(x,y), \psi_{j,k,m}^3(x,y)\}_{k,m\in Z}$ respectively form Riesz bases of V_j^2 and W_j^2.

Since $V_j^2 = V_{j-1}^2 \oplus W_{j-1}^2$, there must be the orthogonal projections of $f_j(x,y)\in V_j^2$ respectively onto $f_{j-1}(x,y)\in V_{j-1}^2$ and $r_{j-1}(x,y)\in W_{j-1}^2$. Thus $f_j(x,y)$ can be represented as

$$f_j(x,y) = \sum_{k,m} c_{k,m}^j \phi_{j,k,m} = f_{j-1}(x,y) + r_{j-1}(x,y). \tag{14}$$

Here

$$\begin{cases} f_{j-1}(x,y) = \sum_{k,m} c_{k,m}^{j-1}\phi_{j-1,k,m} \\ r_{j-1}(x,y) = \sum_{k,m} d_{k,m}^{j-1,1}\psi_{j-1,k,m}^1 + \sum_{k,m} d_{k,m}^{j-1,2}\psi_{j-1,k,m}^2 \\ \qquad + \sum_{k,m} d_{k,m}^{j-1,3}\psi_{j-1,k,m}^3 \end{cases}, \tag{15}$$

with $\{c_{k,m}^j\}_{k,m\in Z}$, $\{d_{k,m}^{j-1,1}\}_{k,m\in Z}$, $\{d_{k,m}^{j-1,2}\}_{k,m\in Z}$ and $\{d_{k,m}^{j-1,3}\}_{k,m\in Z} \in l^2$.

On the other hand, there exists a filter bank $(P(w), Q(w))$ corresponding to scaling function $\phi(x)$ and wavelet $\psi(x)$, which satisfies

$$\begin{cases} \hat{\phi}(w) = P(w)\hat{\phi}(w/2) \\ \hat{\psi}(w) = Q(w)\hat{\phi}(w/2) \end{cases}. \tag{16}$$

Their corresponding dual low-pass and high-pass filters are

$$\begin{cases} G(w) = \sum_{k=-\infty}^{+\infty} g_k e^{-iwk/2} \\ H(w) = \sum_{k=-\infty}^{+\infty} h_k e^{-iwk/2} \end{cases}, \tag{17}$$

where $\{g_k\}_{k\in Z}$, $\{h_k\}_{k\in Z} \in l^2$. Then the two-dimensional Mallat pyramidal algorithm can be expressed

as

$$\begin{cases} c_{k,m}^{j-1} = \sum_l \sum_n g_{l-2k} g_{n-2m} c_{l,n}^j \\ d_{k,m}^{j-1,1} = \sum_l \sum_n g_{l-2k} h_{n-2m} c_{l,n}^j \\ d_{k,m}^{j-1,2} = \sum_l \sum_n h_{l-2k} g_{n-2m} c_{l,n}^j \\ d_{k,m}^{j-1,3} = \sum_l \sum_n h_{l-2k} h_{n-2m} c_{l,n}^j \end{cases}. \tag{18}$$

From (18), wavelet coefficients $\{c_{l,n}^j\}$ of an image can be decomposed into four subsets as $\{c_{k,m}^{j-1}\}$, $\{d_{k,m}^{j-1,1}\}$, $\{d_{k,m}^{j-1,2}\}$, $\{d_{k,m}^{j-1,3}\}$. Since $\{g_k\}_{k\in Z}$ and $\{h_k\}_{k\in Z}$ are low-pass and high-pass filters, $\{d_{k,m}^{j-1,1}\}$ describes the vertical edge of an image. Similarly, $\{d_{k,m}^{j-1,2}\}$ and $\{d_{k,m}^{j-1,3}\}$ respectively describe edges in horizontal and diagonal directions[1]. Equation (18) implies that image edges can be detected only if the wavelet coefficients $\{c_{l,n}^j\}$ and filter sequences $\{g_k\}_{k\in Z}$, $\{h_k\}_{k\in Z}$ are obtained.

The Properties of Interpolation Wavelet

Let $S^{\phi}(x)$ and $S^{\psi}(x)$ respectively denote the interpolation scaling function and the interpolation wavelet. From [11], we have the unique series expressions

$$f_s(x) = \sum_{k\in Z} f_s(k/2^j) S^{\phi}(2^j x - k) \tag{19}$$

and

$$r_s(x) = \sum_{k\in Z} r_s(k/2^j + 1/2^{j+1}) S^{\psi}(2^j x - k) \tag{20}$$

with $f_s(x) \in V_j$ and $r_s(x) \in W_j$, $j \in Z$. It follows from (19) and (20) that $S^{\phi}(x)$ and $S^{\phi}(x)$ are respectively special scaling function and wavelet with coefficients in terms of $\{f_s(k/2^j)\}_{k\in Z}$ and $\{r_s(k/2^j + 1/2^{j+1})\}_{k\in Z}$.

The properties of interpolation wavelets as in (19) and (20) can be easily extended to two-dimensional case. Suppose that $S^{\phi}(x,y) = S^{\phi}(x)S^{\phi}(y)$ and

$$\begin{cases} S^{\psi 1}(x,y) = S^{\phi}(x)S^{\psi}(y) \\ S^{\psi 2}(x,y) = S^{\psi}(x)S^{\phi}(y) \\ S^{\psi 3}(x,y) = S^{\psi}(x)S^{\psi}(y) \end{cases} \tag{21}$$

respectively denote two-dimensional interpolation scaling function and wavelets in spaces V_0^2 and W_0^2. According to wavelet theory, $\{S_{j,k,m}^{\phi}(x,y)\}_{k,m\in Z}$ and $\{S_{j,k,m}^{\psi 1}(x,y), S_{j,k,m}^{\psi 2}(x,y), S_{j,k,m}^{\psi 3}(x,y)\}_{k,m\in Z}$ respectively form a Riesz basis in V_j^2 and W_j^2. Thus, we have two-dimensional series expressions

$$\begin{aligned} f_s(x,y) &= \sum_{k,m} f_s(k/2^j, m/2^j) S^{\phi}(2^j x - k, 2^j y - k) \\ r_s(x,y) &= \sum_{k,m} r_s(k/2^j, m/2^j + 1/2^{j+1}) S^{\psi 1}(2^j x - k, 2^j y - k) \\ &\quad + \sum_{k,m} r_s(k/2^j + 1/2^{j+1}, m/2^j) S^{\psi 2}(2^j x - k, 2^j y - k) \\ &\quad + \sum_{k,m} r_s(k/2^j + 1/2^{j+1}, m/2^j + 1/2^{j+1}) \\ &\quad * S^{\psi 3}(2^j x - k, 2^j y - k) \end{aligned} \tag{22}$$

for any functions $f_s(x,y) \in V_j^2$ and $r_s(x,y) \in W_j^2$.

Moreover, equations (22) implies that sampling values are interpolation wavelet coefficients. This reminds us to decompose images via Mallat pyramidal algorithm. Assume that low-pass and high-pass interpolation filters are

$$\begin{cases} P_s(w) = \sum_{k=-\infty}^{+\infty} p_k^s e^{-iwk/2} \\ Q_s(w) = \sum_{k=-\infty}^{+\infty} q_k^s e^{-iwk/2} \end{cases} \tag{23}$$

with $\{q_k^s\}_{k\in Z}$, $\{p_k^s\}_{k\in Z} \in l^2$. Their corresponding dual filters are

$$\begin{cases} G_s(w) = \sum_{n=-\infty}^{+\infty} g_n^s e^{-iwn/2} \\ H_s(w) = \sum_{n=-\infty}^{+\infty} h_n^s e^{-iwn/2} \end{cases} \tag{24}$$

with $\{g_n^s\}_{n\in Z}$, $\{h_n^s\}_{n\in Z} \in l^2$. Clearly pixel values of images are interpolation wavelet coefficients. Hence, image edges can be detected even without integral formula as in (4) if Mallat pyramidal algorithm (18) is applied to $(P_s(w), Q_s(w))$ and $(G_s(w), H_s(w))$ as in (13) and (14).

In the following, we will show how to obtain interpolation filters. From wavelet theory, $P_s(w)$ and $Q_s(w)$ satisfy

$$\begin{cases} \hat{S}^{\phi}(w) = P_s(w)\hat{S}^{\phi}(w/2) \\ \hat{S}^{\psi}(w) = Q_s(w)\hat{S}^{\phi}(w/2) \end{cases}, \tag{25}$$

where $\hat{S}^{\phi}(w)$ and $\hat{S}^{\psi}(w)$ are the Fourier transforms of $S^{\phi}(x)$ and $S^{\psi}(x)$. It is derived from (25) that

$$P_s(w) = \sum_{k=-\infty}^{+\infty} \hat{S}^{\phi}(w+4k\pi). \tag{26}$$

Equation (26) implies that $P_s(w)$ can be considered as the form of $\hat{S}^{\phi}(w)$. It is shown in [10] that

$$\hat{S}^{\phi}(w) = \frac{\hat{\phi}(w)}{\sum_{k=-\infty}^{+\infty} \hat{\phi}(w+2k\pi)}, \tag{27}$$

where $\hat{\phi}(w)$ is the Fourier transform of a scaling function $\phi(x)$. Inserting (27) into (26) yields

$$P_s(w) = \sum_{k=-\infty}^{+\infty} \frac{\hat{\phi}(w+4k\pi)}{\sum_{k=-\infty}^{+\infty} \hat{\phi}(w+6k\pi)}, \tag{28}$$

(28) implies that the low-pass filter $P_s(w)$ can be obtained via scaling function $\hat{\phi}(w)$.

By [11], the high-pass filter $Q_s(w)$ can be expressed in terms of $P_s(w)$ and $E_s(w)$ as

$$Q_s(w) = \frac{e^{-iw/2} E_s(w+2\pi)\overline{P_s(w+2\pi)}}{\overline{P_s(w+2\pi)}E_s(w+2\pi) + \overline{P_s(w)}E_s(w)}, \tag{29}$$

where $E_s(w) = \sum_{k=-\infty}^{+\infty} \left|\hat{S}^{\phi}(w/2+2k\pi)\right|^2$. (28) and (29) imply that the interpolation filter bank $(P_s(w), Q_s(w))$ can be constructed only if the scaling function $\phi(x)$ is obtained. In addition, from the classical wavelet theory, we have

$$\begin{cases} G_s(w) = \dfrac{Q_s(-w)}{Q_s(-w)P_s(w) - Q_s(w)P_s(-w)} \\ H_s(w) = \dfrac{P_s(-w)}{Q_s(w)P_s(-w) - P_s(w)Q_s(-w)} \end{cases}. \tag{30}$$

Equation (30) has supplied an effective method for constructing the corresponding dual filter bank $(G_s(w), H_s(w))$ from $(P_s(w), Q_s(w))$, which is basic for using Mallat pyramidal algorithm to detect image edges.

Edge detection algorithm based on interpolation wavelet

Two-dimensional Interpolation Wavelet Decomposition

In this section, we apply interpolation filters to Mallat pyramidal algorithm, and discuss interpolation wavelet decomposition algorithm for images.

From (22), (15) can be further expressed as

$$\begin{aligned} f_{j-1}(x,y) &= \sum_{k,m} f_{j-1}(k/2^{j-1}, m/2^{j-1}) S^{\phi}(2^{j-1}x-k, 2^{j-1}y-k) \\ r_{j-1}(x,y) &= \sum_{k,m} r_{j-1}(k/2^{j-1}, m/2^{j-1}+1/2^{j}) S^{\psi 1}(2^{j-1}x-k, 2^{j-1}y-k) \\ &\quad + \sum_{k,m} r_{j-1}(k/2^{j-1}+1/2^{j}, m/2^{j-1}) S^{\psi 2}(2^{j-1}x-k, 2^{j-1}y-k) \\ &\quad + \sum_{k,m} r_{j-1}(k/2^{j-1}+1/2^{j}, m/2^{j-1}+1/2^{j}) \\ &\quad * S^{\psi 3}(2^{j-1}x-k, 2^{j-1}y-k) \end{aligned}. \tag{31}$$

Compared (15) to (31), we have

$$\begin{cases} c_{k,m}^{j-1} = f_{j-1}(k/2^{j-1}, m/2^{j-1}) \\ d_{k,m}^{j-1,1} = r_{j-1}(k/2^{j-1}, m/2^{j-1}+1/2^{j}) \\ d_{k,m}^{j-1,2} = r_{j-1}(k/2^{j-1}+1/2^{j}, m/2^{j-1}) \\ d_{k,m}^{j-1,3} = r_{j-1}(k/2^{j-1}+1/2^{j}, m/2^{j-1}+1/2^{j}) \end{cases}. \tag{32}$$

(32) implies that sampling values of $f_{j-1}(x,y)$ and $r_{j-1}(x,y)$ in their row and column directions can be considered as wavelet coefficients, which are crucial for implementing interpolation wavelet decomposition algorithm.

Let $f_J(x,y)$ denotes an image. Clearly, $f_J(x,y)$ is an energy limited function. According to multi-resolution analysis theory, there exists an approximation space $V_J \subset \{V_j\}_{j\in Z}$ such that $f_J(x,y) \in V_J$, where J is a fixed scale. From sampling theory, image with a size of $N_1 \times N_2$ also can be expressed as a matrix $A_{map} = [a_{k,m}]_{N_1 \times N_2}$, where $a_{k,m} = f_J(k/2^J, m/2^J)$ forms gray value at coordinate point (k,m). From (32), we have

$$c_{k,m}^{J} = f_J(k/2^J, m/2^J). \tag{33}$$

Equation (33) implies that the pixel matrix A_{map} of a digital image can be considered as wavelet coefficients $\{c_{k,m}^J\}$. Thus, the wavelet coefficients of images can be obtained quickly.

Since the number of pixels is limited, coordinates of the image pixels can be depicted in Fig.1.

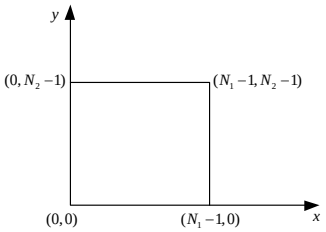

Fig. 1. Four vertexes of an image

Hence, from (18) and (32), the interpolation wavelet decomposition algorithm can be expressed as

$$\begin{cases} f_{J-1}(k/2^{J-1}, m/2^{J-1}) = \\ \sum_{l=0}^{N_1-1}\sum_{n=0}^{N_2-1} g_{l-2k}^{s} g_{n-2m}^{s} f_J(l/2^J, n/2^J) \\ r_{J-1}(k/2^{J-1}, m/2^{J-1}+1/2^J) = \\ \sum_{l=0}^{N_1-1}\sum_{n=0}^{N_2-1} g_{l-2k}^{s} h_{n-2m}^{s} f_J(l/2^J, n/2^J) \\ r_{J-1}(k/2^{J-1}+1/2^J, m/2^{J-1}) = \\ \sum_{l=0}^{N_1-1}\sum_{n=0}^{N_2-1} h_{l-2k}^{s} g_{n-2m}^{s} f_J(l/2^J, n/2^J) \\ r_{J-1}(k/2^{J-1}+1/2^J, m/2^{J-1}+1/2^J) = \\ \sum_{l=0}^{N_1-1}\sum_{n=0}^{N_2-1} h_{l-2k}^{s} h_{n-2m}^{s} f_J(l/2^J, n/2^J) \end{cases}, \tag{34}$$

where $\{g_n^s\}_{n\in Z}$, $\{h_n^s\}_{n\in Z}$ are interpolation dual filters as in (24). Suppose that

$$\begin{cases} f_J^s = \left\{ f_J(k/2^J, m/2^J) \right\} \\ r_{J-1,1}^s = \left\{ r_{J-1}(k/2^{J-1}, m/2^{J-1}+1/2^J) \right\} \\ r_{J-1,2}^s = \left\{ r_{J-1}(k/2^{J-1}+1/2^J, m/2^{J-1}) \right\} \\ r_{J-1,3}^s = \left\{ r_{J-1}(k/2^{J-1}+1/2^J, m/2^{J-1}+1/2^J) \right\} \end{cases}. \tag{35}$$

It follows from (34) that the pixel matrix f_J^s can be decomposed into four coefficients as f_{J-1}^s, $r_{J-1,1}^s$, $r_{J-1,2}^s$ and $r_{J-1,3}^s$ only if $\{g_n^s\}$ and $\{h_n^s\}$ are obtained.

It follows from wavelet theory that f_{J-1}^s denotes an approximation of image. Simultaneously, $r_{J-1,1}^s$, $r_{J-1,2}^s$ and $r_{J-1,3}^s$ respectively form vertical, horizontal and diagonal image edges. By recursively applying (34) to f_{J-1}^s, we can get a series of edge images with different resolutions.

Edge Detection Algorithm

Based on the discussions abovementioned, the new edge detection algorithm can be described in the following steps.

Step1: Inserting a scaling function $\hat{\phi}(w)$ into (27) gives an interpolation scaling function $\hat{S}^{\phi}(w)$. Hence, low-pass and high-pass interpolation filter bank $(P_s(w), Q_s(w))$ can be constructed from $\hat{S}^{\phi}(w)$ by (26) and (29). From (30), the corresponding dual filter bank $(G_s(w), H_s(w))$ can be get via $(P_s(w), Q_s(w))$, which means filter sequences g^s and h^s are obtained.

Step2: Setting a scale as J, then inserting the image pixel matrix f_J^s and the filter bank (g^s, h^s) into (34) yields decomposition coefficients f_{J-1}^s and $r_{J-1,1}^s$, $r_{J-1,2}^s$, $r_{J-1,3}^s$.

Step3: If the resolution of image edges from step2 can't meets our requirements, we can recursively decompose f_{J-1}^s until coefficients $r_{J-M,1}^s$, $r_{J-M,2}^s$, $r_{J-M,3}^s$ with a desired resolution are obtained.

Step4: Inserting $r_{J-M,1}^s$, $r_{J-M,2}^s$, $r_{J-M,3}^s$ into

$$d_{J-M}^s = \sqrt{{r_{J-M,1}^s}^2 + {r_{J-M,2}^s}^2 + {r_{J-M,3}^s}^2}, \tag{36}$$

we can get a matrix d_{J-M}^s which can reflect integrated edges of an image.

Step5: Selecting a suitable threshold T, then the edges can be obtained by choosing coefficients in d_{J-M}^s are greater than T.

The above-mentioned process can be shown as Fig.2.

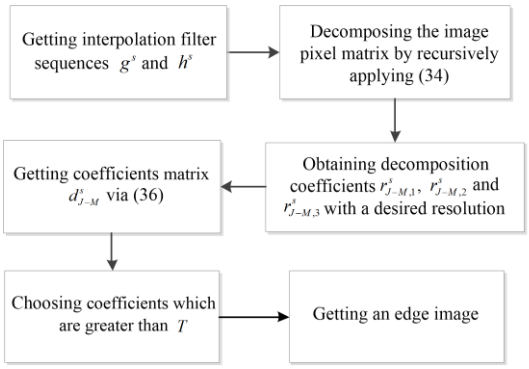

Fig. 2. Flow chart of edge detection algorithm

It follows from Fig.2 that our algorithm can get wavelet coefficients directly from image pixels. Compared to the classic wavelet algorithm, in which wavelet coefficients have to be obtained via integral formulas, our algorithm can detect image edges simply and accurately.

Experiment Results and Analyses

In this section, we choose a pears image and a more complex lena image as original images, which are shown in Fig. 3. Edge detection results of the sobel operator[6], the classic wavelet algorithm, and the multiscale edge detection algorithm in [4] would be compared with result of our algorithm.

This experiment uses a sixth order spline wavelet for classic wavelet algorithm and our algorithm. Edge detection results with $J = -2$ are depicted in Fig.4~5.

(a) PEARS (b) LENA

Fig. 3. Original images

As is shown in Fig.4(a), edges detected by sobel operator is clear but not intact. The classic wavelet algorithm has detected a blurry edge image (Fig.4(b)) with many discontinuous edges and few details. Edges detected by algorithm in [4] (Fig.4(c)) also exist many breakpoints. However, as we can see in Fig.4(d), the detect result of our algorithm has a continuous and intact edge image with less textures, which is better than three algorithms above.

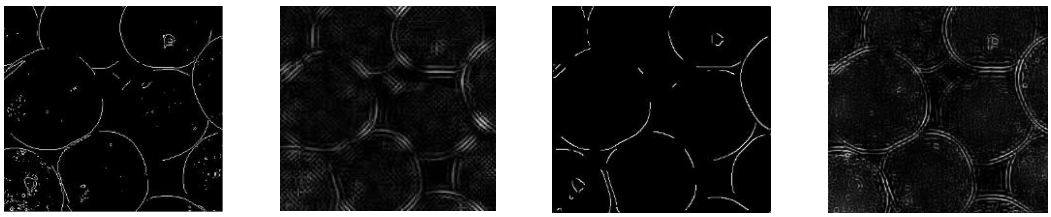

(a) Sobel edge detector (b) Classic wavelet algorithm (c) Algorithm in [4] (d) Our algorithm

Fig. 4. Detect results of PEARS

When detect a more complex lena image, from Figure 5(a)~(c), we can see that lots of discontinuous edges are detected by the sobel operator. Simultaneously, the classic wavelet algorithm and the algorithm in [4] also have poor results when it comes to edges with lower contrast. Both of three algorithms can only obtain a crude outline, and have difficulties in detecting complicated details. But as is shown in Fig.5(d), the edge image detected by our algorithm has accurate locations and clear descriptions of hair and decorations on the hat. Furthermore, details of eyes and nose also can be preserved well in the result of our algorithm.

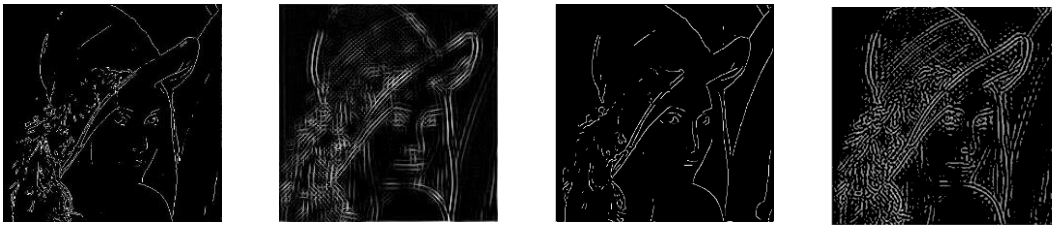

(a) Sobel edge detector (b) Classic wavelet algorithm (c) Algorithm in [4] (d) Our algorithm

Fig. 5. Detect results of LENA

From the theoretical analysis abovementioned, we know that in classic wavelet algorithm, there is a contradiction between the resolution of image edge detection and the solving accuracy of wavelet coefficients. This leads up to the unsatisfactory edge detection result. In our algorithm, since wavelet coefficients are obtained via interpolation wavelet decomposition, this method overcomes the influence of integral formula in classic wavelet algorithm. Experimental results as shown in Fig. 4 and Fig. 5 fully verify the effectiveness of our algorithm.

Conclusion

This paper proposed a new edge detection algorithm based on interpolation wavelet pyramid decomposition. This has solved the problem that the classic wavelet algorithm generally cannot obtain precise wavelet coefficients and fine resolution at the same time. The experimental results

demonstrate that the new algorithm has a stronger detection capacity of details and improves the location accuracy. Thus a better edge result can be obtained.

Acknowledgement

This research was financially supported by “the Fundamental Research Funds for the Central University”.

References

[1] MALLAT S, ZHONG S. Characterization of signals from multiscale edges. IEEE Trans on Pattern and Machine Intelligence, 1992, 14(7): 710-732.

[2] MALLAT S, HWANG W L. Singularity detection and processing with wavelets. IEEE Trans on Information Theory, 1992, 38(2): 617-643.

[3] KOBYLIN O, LYASHENKO V. Comparison of standard image edge detection techniques and of method based on wavelet transform. International Journal of Advanced Research, 2014, 2(8): 572-580.

[4] SHAO Ting-ting, BAI Zong-wen, ZHOU Mei-li. Image edge detection based on wavelet transform. Electronic Test, 2014, 19: 26-27. (in Chinese).

[5] CHO W, JEON J. Edge detection in wavelet transform domain. Frontiers of Computer Vision, 2015:1-4.

[6] LI Zhe-tao, LI Ren-fa, XIE Jin-xiong. An edge detection algorithm based on omnidirectional wavelet transform. ACTA ELECTRONICASINICA, 2012, 12: 2451-2455. (in Chinese).

[7] YUE Ming-ming, YANG Guo-wei. Multiscale edge detetion algorithm based on modulus maxima of B-spline wavelet tansform. Industrial Control Computer, 2016, 29(9): 108-112. (in Chinese).

[8] LI Zhi, ZHANG Gen-yao, WANG Bei. Medical image edge detection based on wavelet transform and morpholopy. Information Technology, 2015, 4: 84-86. (in Chinese).

[9] SUN Kang-tai, YI Xun-ming, FANG Zhuang. Wavelet threshold denoising method based on canny operator edge detection. J. of Math, 2015, 35(6): 1389-1392. (in Chinese).

[10] WALTER G G. A sampling theorem for wavelet subspaces. IEEE Transactions on Information Theory, 1992, 38(2): 881-884.

[11] ZHANG Z G, KON M A. On relating interpolatory wavelets to interpolatory scaling functions in multiresolution analyses. Circuits, Systems, and Signal Proccessing, 2015, 34(6): 1947-1976.